JOURNAL OF Materials CHEMISTRY

Ionic conduction of lithium in B-site substituted perovskite compounds, $(Li_{0.1}La_{0.3})_yM_xNb_{1-x}O_3$ (M = Zr, Ti, Ta)

Masanobu Nakayama, Hiromasa Ikuta, Yoshiharu Uchimoto and Masataka Wakihara*

Department of Chemical Engineering, Tokyo Institute of Technology, Ookayama, Meguro-ku, Tokyo 152-8552, Japan. E-mail: mwakihar@o.cc.titech.ac.jp; Fax: +81 3 5734 2146; Tel: +81 3 5734 2145

Received 9th January 2002, Accepted 21st February 2002
First published as an Advance Article on the web 26th March 2002

Dependence of the lattice parameter and Li^+ ionic conductivity on the B-site ion substitution in perovskite-related compounds $(Li_{0.1}La_{0.3})_yM_xNb_{1-x}O_3$ (M = Zr, Ti, Ta) has been investigated. According to the calculation based on the classical ionic crystal model, ionic conductivity is expected to increase under the following two conditions: (i) a smaller average charge of B-site cations; and (ii) a larger unit cell. From the powder XRD results, Zr^{4+} substitution was satisfied with these two conditions. While in the case of Ti^{4+} substitution the former condition was satisfied, the latter one showed opposite tendency. In the case of Ta^{5+} substitution, both of the conditions are not changed. Therefore Zr^{4+}-substituted samples were expected to increase the ionic conductivity. However, the ionic conductivity of all the B-site substituted samples decreased with the amount of substitution, in particular, Zr^{4+}-substituted samples showed the lowest ionic conductivity. This disagreement indicates that there is an additional factor affecting the ionic conductivity. We suggest three possible explanations: (1) local distortion introduced by cation substitution; (2) the change of B–O bond covalency; and (3) formation of short-range ordering with B-site substitution.

Introduction

Development of materials with an ionic conductivity as high as lithium is important in order to improve the performance of solid state secondary batteries. From the process of exploring such materials, there have been several reports on perovskite oxides containing Li^+ ions. In particular, lanthanum lithium titanate, having a perovskite structure, exhibits a fairly high ionic conductivity (*ca.* 10^{-3} S cm^{-1} at room temperature).[1–4] Also, Latie *et al.*[5] have investigated the Li^+ ionic conductivity in the $Li_xLn_{1/3}Nb_{1-x}Ti_xO_3$ (Ln = La, Nd), and these materials show a value of *ca.* 10^{-5} S cm^{-1} at room temperature. Such high conductivities of these perovskite-type materials is considered as coming from the presence of a large number of vacancies on the A-sites and a large number of equivalent sites for the lithium ion to move freely within the A-site space of the perovskite.

The perovskite-related compounds $Ln_{1/3}NbO_3$ (Ln = rare earth ion) have a relatively unique crystal structure which was first described by Iyer and Smith[6] and later by Trunov *et al.*[7] According to such literature, the NbO_3 framework is made up of NbO_6 octahedra sharing B-sites, and Ln ions and vacancy sites are alternately stacked at the A-sites along the *c*-axis (Fig. 1). By substitution of $3Li^+$ for Ln^{3+}, this material exhibits lithium ionic conduction. Several works have been focused on the ionic conductivity and crystal structure of the compounds expressed by the general formula $La_{2/3-x}Li_{3x}Nb_2O_6$.[8–11]

In our previous studies,[10,12] we investigated the relationship between crystal structure and ionic conductivity for these perovskite compounds in which La^{3+} ions in the A-sites were replaced by larger Sr^{2+} and smaller Ca^{2+} ions. The activation energy of ionic conduction tends to decrease with increasing perovskite parameter a_p (lattice parameter of perovskite structure regarded as a cubic lattice) (Fig. 2). These results indicate that the ionic conduction is strongly affected by the size of bottle-neck area which is the smallest cross-sectional area of conducting passageway.

In the present paper, we have synthesized three perovskite compounds with different substitution cations in the B-sites $(Li_{0.1}La_{0.3})_yM_xNb_{1-x}O_3$ (M = Zr, Ti, Ta) and investigated the relationship between the crystal structure and the lithium ionic conductivity in view of the classical ionic crystal model.

Model

It was assumed that this perovskite belongs to the classical ionic crystal which is composed of ionic bonds between cations and anions. Therefore the variation of potential energy through the ionic conduction can be understood by the combination of the Coulombic potential and the repulsive potential arising from electron orbital overlapping [eqn. (1)],

$$U_i = \sum_{j \neq i} \frac{1}{4\pi\varepsilon_0} \frac{Z_i Z_j e^2}{r_{ij}} + \sum_{j \neq i} \frac{\lambda}{r_{ij}{}^n} \quad (1)$$

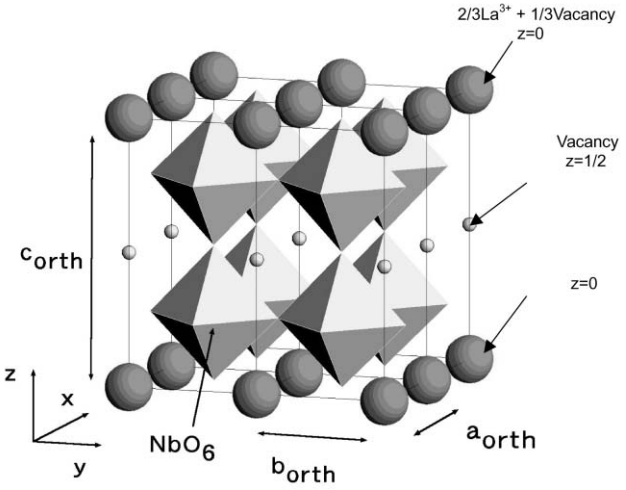

Fig. 1 The structure of $La_{1/3}NbO_3$.

 DOI: 10.1039/b200310d

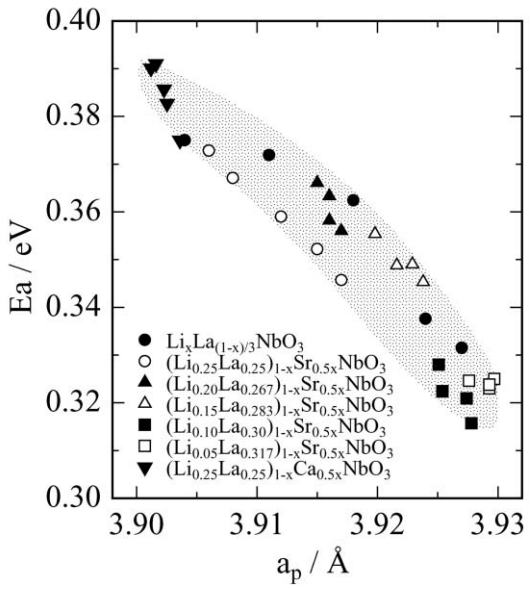

Fig. 2 Variation of the activation energy of lithium ion conduction in perovskite structure *versus* perovskite parameter a_p (p refers to the perovskite unit cell).

where U_i indicates the potential energy of ions i, ε_0 means dielectric constant in a vacuum, Z_i means ionic charge of ion i, r_{ij} is the interionic distance between ions i and j, λ and n are the constant values depending on adjacent ion pairs. The first term of this equation is expressed as a Coulombic potential, and the latter term corresponds to the repulsive potential. Accordingly, by considering only two parameters, r_{ij} and Z_j, the variation of ionic conductivity with B-site substitution can be estimated.

Simplifications of the estimation for the ionic conductivity behavior can be achieved in investigating how the charge distribution affects the ionic conductivity under the same lattice size. In other words, the value of r_{ij} was fixed, and the variation of potential energy *versus* the average charge of B-site cations was calculated. In this situation, a second repulsive term is constant and it is sufficient to pay attention only to the variation of the first term of Coulombic potential. Fig. 3 shows the variation of the calculated Coulombic energy of lithium along the straight line between two A-sites [see Fig. 3(a)] *versus* the average charge of the B-site, Z_B. In this calculation, the crystal structure parameters were cited from the data in ref. 6, and the charge neutrality was satisfied by adjusting the average charge of the A-site cations. Potential energy of Li^+ shows the largest value at the bottle-neck site and the smallest value at the A-site in the Z_B = *ca.* +5.0 to +4.8 region. This potential difference, which corresponds to the activation energy, E_a, decreases with the decrease of the average cation charge in the B-sites. Therefore the ionic conductivity is expected to increase with any decrease in the B-site cation charge.

Next we examined lattice size effect on the conductivity under the same charge distribution in the perovskite structure. That is to say, the value of Z_j in eqn. (1) is fixed, and the variation of potential energy U_i *versus* r_{ij} is investigated (the value of r_{ij} directly corresponds to the unit cell size). The potential energy of Li^+ is the largest (unstabilized) at the bottle-neck through the Li^+ ion conducting pathway, since the second repulsive term due to electron orbital overlapping between Li^+ and O^{2-} ions might be a predominant factor. In such a case, the activation energy E_a is expressed as the potential energy change between the A-site positions and bottle-neck position [E_a = U(bottle-neck) − U(A-site)]. From this point of view, the activation energy E_a is mainly caused by the second repulsive term and is led to decrease with increasing r_{ij}. Our previous results shown in Fig. 2 supported this idea experimentally [the data were obtained under the same B-site

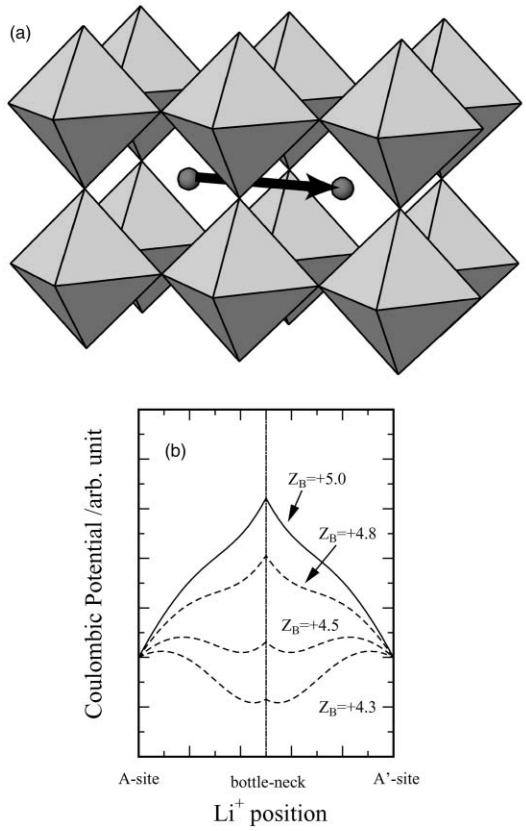

Fig. 3 Variation of the calculated Coulombic potential energy with Li^+ position *versus* average charge of the B-site: (a) the calculated Li^+ position which migrates along the arrow line from A-site to A′-site; (b) the calculated results.

valence (Z_j) and various r_{ij} parameters]. Therefore, the ionic conductivity is expected to increase with expansion of lattice.

Accordingly, the ionic conductivity of lithium would increases under following two conditions:

(i) a smaller average charge in the B-site;

(ii) a larger lattice parameter.

Experimental

Samples of $(Li_{0.1}La_{0.3})_yM_xNb_{1-x}O_3$ substituted at the B-site (M = Zr^{4+}, Ti^{4+}, Ta^{5+}; y is arranged by considering the electrical neutrality requirement) were synthesized by conventional solid state reaction. Reagents of Li_2CO_3 (Soekawa Chem. Co., Ltd. 99.9%), La_2O_3 (Soekawa Chem. Co., Ltd. 99.9%), Nb_2O_5 (Soekawa Chem. Co. Ltd., 99.9%), ZrO_2 (Soekawa Chem. Co. Ltd., 99.9%), TiO_2 (anatase, Soekawa. Chem. Co. Ltd., 99.98%), Ta_2O_5 (Soekawa Chem. Co. Ltd., 99.9%) were used as starting materials. La_2O_3 was preheated at 1000 °C in order to remove absorbed CO_2. Stoichiometric amounts of starting reagents were mixed in an agate mortar with ethanol. The mixture was pelletized and heated at 800 °C for 2 h and then at 1250 °C for 24 h in Pt crucible under an air atmosphere with several intermittent grindings.

The samples were characterized by the powder XRD technique using a Rigaku RINT2500V with CuKα radiation which was monochromatized by a curved crystal of graphite. The XRD data for determination of the lattice parameters were collected in the 2θ range of 60–100° with a step width of 0.01°. Silicon was used as an external standard in the determination of the lattice parameters.

Ionic conductivity for the bulk of the sample was measured by an AC impedance technique. Specimens with two electrodes for conductivity measurement were prepared as follows. The powder samples were pressed into a pellet of 6 mm diameter

and 1 mm thickness under a pressure of 20 MPa, and the pellet was sintered at 1250 °C for 12 h. The porosities of all of the obtained pellets were ca. 6–7%. After sintering, the surface of the pellets was polished with emery paper, the pellets were then washed in acetone using an ultrasonic cleaner and dried at 110 °C under vacuum. Gold was sputtered on to both sides of the pellet in order for use as the electrodes. Complex impedance was measured using an L.F. impedance analyzer HP4192A over the temperature range from 20 to 300 °C at frequencies from 5 Hz to 13 MHz.

Results

Fig. 4 shows the powder XRD patterns of solid-solution $(Li_{0.1}La_{0.3})_yZr_xNb_{1-x}O_3$ ($0 \leqslant x \leqslant 0.075$) samples. Under our experimental conditions, the only perovskite phase was observed in the composition range from $x = 0$ to 0.05, while weak peaks due to $LaNbO_4$ and an unknown impurity phase were observed with the composition of x larger than 0.0625. Similarly, the single phase regions were determined as $x \leqslant 0.075$ for Ti substitution and $x \leqslant 0.0625$ for Ta substitution. Lattice parameters of these samples are shown in Fig. 5. According to Belous *et al.*[8] and from our previous research,[10] the crystal system changed from orthorhombic to tetragonal and then to cubic with an increasing fraction of Li in the A-site. In this study, the X-ray diffraction peaks of all the samples could be indexed in a tetragonal system, and there were no peak splits due to orthorhombic distortion.

Both the lattice parameters (Fig. 5) and the cell volume (Fig. 6) of the samples replaced by B-site cations change linearly with increasing composition of x. The partial substitution of Zr^{4+} for Nb^{5+} caused an increase of the cell volume, while that of Ti^{4+} for Nb^{5+} caused a decrease. In the case of the partial substitution of Ta^{5+} for Nb^{5+}, no marked change in the cell volume was observed. Comparing the ionic radius[13] of substituting ions, Zr^{4+}(0.72 Å), Ti^{4+}(0.605 Å), and Ta^{5+}(0.64 Å) with that of the host ion Nb^{5+} (0.64 Å), the variation of cell volumes for samples substituted at the B-sites depends on the size of the substituting cations. In addition the lattice replaced by tetravalent cations (Zr^{4+} and Ti^{4+}) tends to be elongated along the c-axis. The possible reason for this tendency is the difference of Li^+ distribution in the A-sites, or

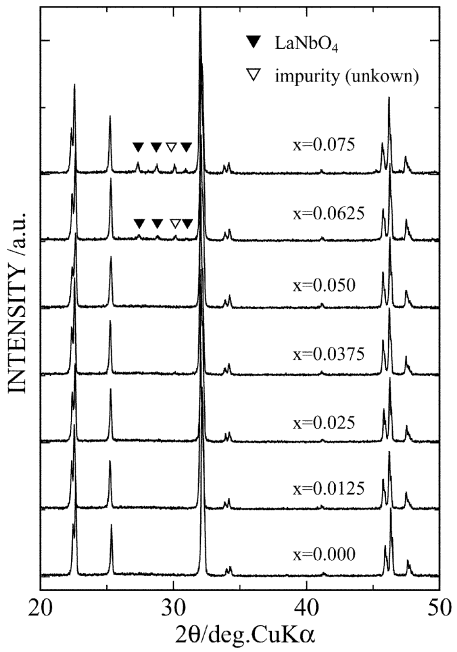

Fig. 4 Powder XRD patterns for $(Li_{0.1}La_{0.3})_{1-x}Zr_xNb_{1-x}O_3$.

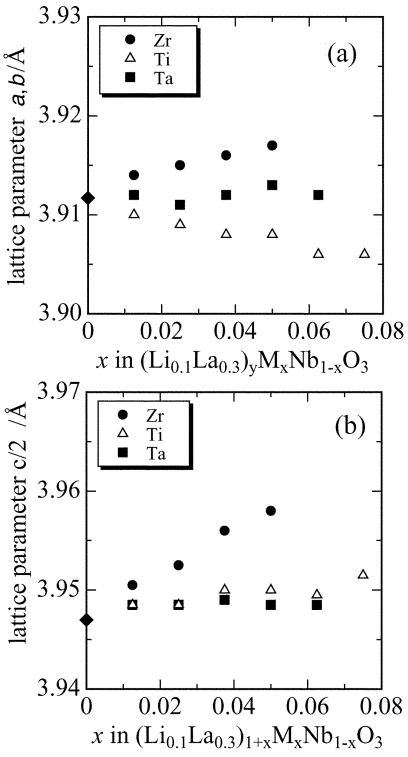

Fig. 5 Variation of lattice parameters *versus* x in $(Li_{0.1}La_{0.3})_yM_xNb_{1-x}O_3$: (a) lattice parameter a, b; (b) lattice parameter $c/2$.

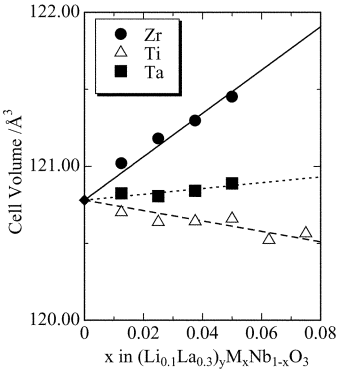

Fig. 6 Variation of cell volume with B-site substitution in $(Li_{0.1}La_{0.3})_yM_xNb_{1-x}O_3$.

the covalency effect between B-site cations and oxide ions. However, the exact reason is still unknown.

Fig. 7 and Table 1 show typical complex impedance plots

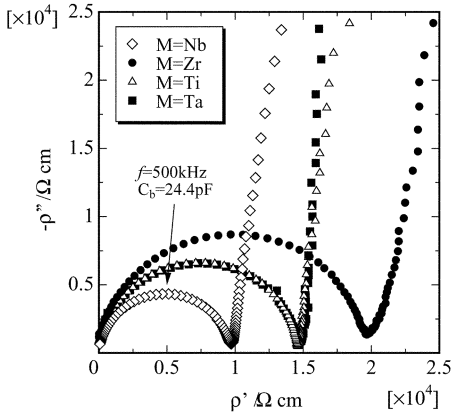

Fig. 7 Typical example of the impedance plots for the samples $(Li_{0.1}La_{0.3})_yM_{0.05}Nb_{0.95}O_3$ (M = Nb, Zr, Ti, Ta).

Table 1 Typical example of the impedance plots for the samples $(Li_{0.1}La_{0.3})_yM_{0.05}Nb_{0.95}O_3$ (M = Nb, Zr, Ti, Ta). Parameters f, ρ_b and C_b indicate frequencies of peak top, relative resistance for the bulk, and capacitance of the bulk samples.

Sample	$Li_{0.1}La_{0.3}NbO_3$	M = Zr	M = Ti	M = Ta
T/°C	43.8	43.9	43.7	40.2
f/kHz	501	355	447	501
ρ_b/Ω cm	9440	19 740	14 800	14 800
C_b/pF	24.4	21.8	21.4	20.0

and data obtained for selected compositions around 40 °C. In all the samples, semicircles were observed at the higher frequency range, and these capacitances were *ca.* 20 pF which corresponds to bulk capacitance.[14] The bulk resistances were derived by applying the least squares method to the semicircles. Activation energy values E_a for the ionic conduction were determined from Arrhenius plots of ionic conductivity (Fig. 8) using the following equation,

$$\sigma T = A \exp(-E_a/k_B T) \quad (2)$$

where A is the pre-exponential parameter and k_B is the Boltzmann constant. Summarizing the results of Arrhenius plot data as a function of the composition x, Fig. 9(a) shows the activation energy at 298 K and Fig. 9(b) shows the ionic conductivity at the same temperature. Ascending the substitution amount at the B-site, the ionic conductivity monotonously decreased. The activation energy of Zr- and Ti-substituted samples increased in that order, while activation energy of Ta-substituted samples showed no marked change compared with the original one, $Li_{0.1}La_{0.3}NbO_3$,

Discussion

In this section, we discuss the experimental results in view of what is mentioned in the second section (Model). There are two factors to improving the ionic conductivity: (i) to decrease the average charge of B-site cation; (ii) to expand the cell volume. Zr^{4+} substitution samples are in agreement with these conditions (see Fig. 6); however, the results of ionic conductivity exhibit an evident decrease (Fig. 9). Comparing the

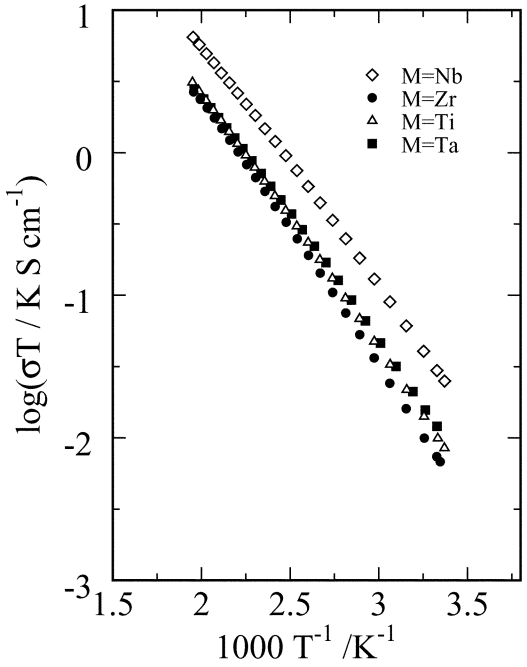

Fig. 8 Typical Arrhenius plots of the ionic conductivity of lithium for the samples $(Li_{0.1}La_{0.3})_yM_{0.05}Nb_{0.95}O_3$ with M = Nb, Zr, Ti, Ta.

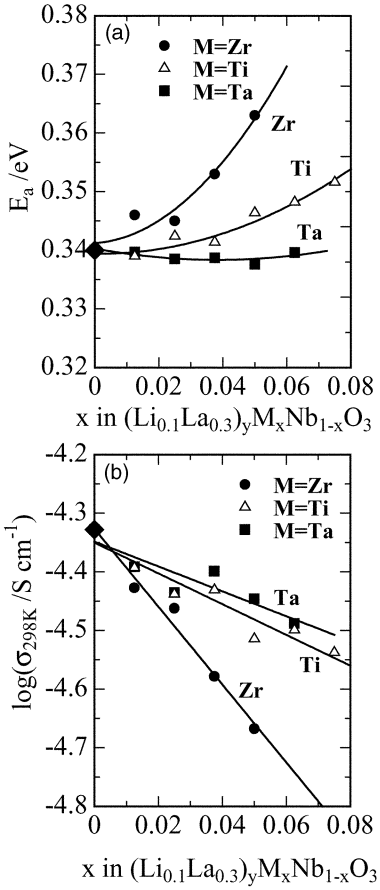

Fig. 9 Variation of (a) the activation energy, and (b) the ionic conductivity, at 298 K with composition x for the perovskite system $(Li_{0.1}La_{0.3})_yM_xNb_{1-x}O_3$.

case of A-site substitution (Fig. 2), the activation energy data for samples substituted at the B-site are replotted as in Fig. 2 and are shown in Fig. 10. The tendency of the relationship between activation energy and lattice parameter for Zr^{4+} substitution are not consistent with previous data, *i.e.* that for A-site substitution. Therefore we conclude that the ionic conductivity of Li^+ in the perovskites substituted with B-site cations cannot be explained by the classical ionic crystal model

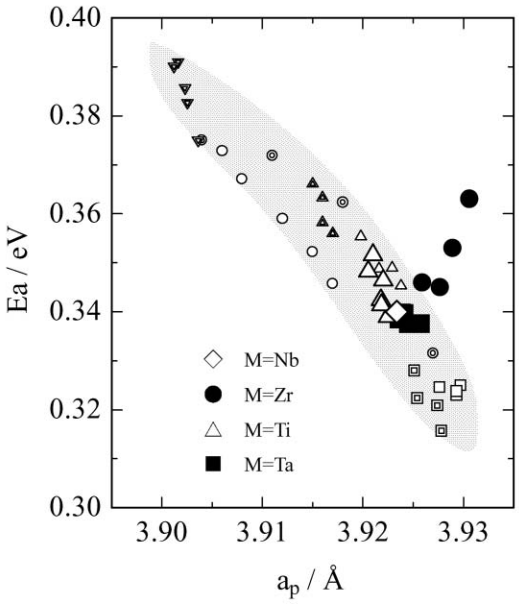

Fig. 10 Variation of the activation energy *versus* perovskite parameter a_p in $(Li_{0.1}La_{0.3})_yM_xNb_{1-x}O_3$ superimposed upon Fig. 2.

alone, but also by another additional model. We suggest three possible mechanisms for our perovskite systems as follows.

(1) First of all, Katsumata *et al.*[15] pointed out the idea of the local distortion effect. The neighboring site of the substituted ion is distorted, and this would cause an increase of the activation energy for ionic migration arising from narrowing of the migration path. This explanation could be applied to our system. Considering ionic radii, the local distortion around a substituted site may increase when the difference of ionic radii between Nb^{5+} (0.64 Å) and substituting ions Zr^{4+} (0.72 Å), Ti^{4+}(0.605 Å), Ta^{5+}(0.64 Å) increases. Such local distortion is expected to raise the activation energy. This scenario is consistent with experimental tendency. This might be one solution to explain the present results.

(2) The second possible reason is that the proposed model described in the Model section does not include a covalent bond effect. Increasing the covalent bond character, the Coulombic interaction between the Li^+ ion and the perovskite framework (BO_3) would decrease, and it can be considered that the resulting ionic conductivity increases. Referring to the electronegativity proposed by Pauling[16] and Allred,[17] values for the B-site cations are 3.5 (O), 1.6 (Nb), 1.54 (Ti), 1.5 (Ta), and 1.33 (Zr). Therefore samples replaced by Zr^{4+} have strong ionic bond character, which leads to the less ionic conduction.

(3) The last possible reason is that B-site substitution enhances the ordering of cations and vacancy in the A-site. García-Martín and Alario-Franco.[18] have recently reported the electron diffraction which includes several satellite reflections in $La_{1/3-x}Li_{3x}NbO_3$. These results may indicate the existence of short-range ordering in the A-site which causes a decrease in ionic conduction. Such an effect has already been reported in an oxide ion conductor (*e.g.* ref. 19). Also, the short-range ordering in the A-site is enhanced by an aliovalent doping because neighboring A-site cations are trapped by lower charged cations. Therefore, the ionic conductivity decreases with B-site substitution.

Conclusion

The lithium ionic conductivity and lattice parameter of B-site substitutution $(Li_{0.1}La_{0.3})_yM_xNb_{1-x}O_3$ (M = Zr, Ti, Ta) have been investigated. In particular, samples replaced with Zr^{4+} show a cell volume expansion and decrease of ionic conductivity with B-site substitution. These results cannot be explained by the pure ionic crystal model mentioned in Model section. Therefore, it is concluded that other possible effects exist. In order to understand the detailed mechanism of the lithium migration process, it is necessary to evaluate local distortion, covalent effects, and the formation of short-range ordering with B-site substitution.

Acknowledgements

This work was supported by Grant-in-Aid for Scientific Research on Priority Areas (B) (No.740) 'Fundamental Studies for Fabrication of All Solid State Ionic Devices' from the Ministry of Education, Culture, Sports, Science and Technology. M. N. would like to thank the New Energy and Industrial Technology Development Organization for financial support of this work.

References

1 Y. Inaguma, L. Chen, M. Itoh, T. Nakamura, T. Uchida, H. Ikuta and M. Wakihara, *Solid State Commun.*, 1993, **86**, 689.
2 Y. Inaguma, L. Chen, M. Itoh and T. Nakamura, *Solid State Ionics*, 1994, **70/71**, 196.
3 M. Itoh, Y. Inaguma, W. H. Jung, L. Chen and T. Nakamura, *Solid State Ionics*, 1994, **70/71**, 203.
4 A. G. Belous, G. N. Novitskaya, S. V. Polyanetskaya and I. Gornikov Yu, *Izv. Akad. Nauk SSSR, Neorg. Mater.*, 1987, 470.
5 L. Latie, G. Villeneuve, D. Conte and G. Le Felm, *J. Solid State Chem.*, 1984, **51**, 293.
6 P. N. Iyer and A. J. Smith, *Acta Crystallogr.*, 1967, **23**, 740.
7 V. K. Trunov, I. M. Averina, A. A. Evdokimov and A. M. Frolov, *Kristallografiya*, 1981, **261**, 189.
8 A. G. Belous, I. R. Didukh, E. B. Novosadova, E. V. Pashkova and B. S. Khomenko, *Izv. Akad. Nauk SSSR, Neorg. Mater.*, 1990, **26**(6), 1294.
9 A. G. Belous, *Solid State Ionics*, 1996, **90**, 193.
10 Y. Kawakami, H. Ikuta and M. Wakihara, *J. Solid State Electrochem.*, 1998, **2**, 206.
11 S. García-Martín, J. M. Rojo, H. Tsukamoto, E. Morán and M. Á. Alario-Franco, *Solid State Ionics*, 1999, **116**, 11.
12 Y. Kawakami, M. Fukuda, H. Ikuta and M. Wakihara, *Solid State Ionics*, 1998, **110**, 187.
13 R. D. Shannon, *Acta Crystallogr., Sect. A*, 1976, **32**, 751.
14 For example, see: J. R. MacDonald, *Impedance Spectroscopy*, Wiley Inter-Science, New York, 1987, ch. 4.
15 T. Katsumata, Y. Matsui, Y. Inaguma and M. Itho, *Solid State Ionics*, 1996, **86–88**, 165.
16 L. Pauling, *The Nature of the Chemical Bond*, Cornell University Press, Ithaca, NY, 3rd edn., 1960.
17 A. L. Allred, *J. Inorg. Nucl. Chem.*, 1961, **17**, 215.
18 S. García-Martín and M. Á. Alario-Franco, *J. Solid State Chem.*, 1999, **148**, 93.
19 J. B. Goodenough, *Solid State Ionics*, 1994, **94**, 17.